

Room-temperature layer-by-layer epitaxial growth and characteristics of Fe_3O_4 ultrathin films

This content has been downloaded from IOPscience. Please scroll down to see the full text.

2014 J. Phys. D: Appl. Phys. 47 105004

(<http://iopscience.iop.org/0022-3727/47/10/105004>)

View [the table of contents for this issue](#), or go to the [journal homepage](#) for more

Download details:

IP Address: 159.226.35.197

This content was downloaded on 20/02/2014 at 06:26

Please note that [terms and conditions apply](#).

Room-temperature layer-by-layer epitaxial growth and characteristics of Fe₃O₄ ultrathin films

Xiangbo Liu, Huibin Lu, Meng He, Le Wang, Hongfei Shi, Kuijuan Jin, Can Wang and Guozhen Yang

Beijing National Laboratory for Condensed Matter Physics, Institute of Physics, Chinese Academy of Sciences, Beijing 100190, People's Republic of China

E-mail: hblu@iphy.ac.cn

Received 30 July 2013, revised 23 December 2013

Accepted for publication 14 January 2014

Published 19 February 2014

Abstract

Fe₃O₄ films with thicknesses of 2–200 unit cells were epitaxially grown on α -Al₂O₃(0001) substrates by laser molecular beam epitaxy at room temperature. The fine streaky pattern and clear intensity oscillations were observed by *in situ* reflection high-energy electron diffraction, indicating that the films are perfect two-dimensional layer-by-layer epitaxial growth. X-ray diffraction and atomic force microscope measurements reveal that the Fe₃O₄ films have high-pure crystal phase and atom-level-smooth surface. The experimental results demonstrate that the structural, electrical and magnetic properties of the room-temperature epitaxial Fe₃O₄ films strongly depend on the film thickness.

Keywords: room-temperature epitaxy, layer-by-layer, Fe₃O₄

(Some figures may appear in colour only in the online journal)

1. Introduction

Room-temperature epitaxial growth of functional film materials has been highly requested from the viewpoint of applications in heterostructures, microelectronic devices and spintronics devices, etc, because it not only avoids atomic interdiffusion at the heterointerface but also reduces the film deterioration and the effects of substrate materials resulting from the thermal treatment. The pulsed laser deposition (PLD) method is an effective way to reduce the growth temperature because the film precursors ablated from the target have high enough kinetic energies to impinge, immigrate and nucleate on the surface, and form epitaxial film further [1]. In recent years, room-temperature epitaxy of some films on well-matched substrates by PLD has been reported, for instance, GaN on ZnO [2], InAlN on ZnO [3], AlN on SiC [4], GaN on ZrB₂ [5]. In some cases, epitaxial films can grow in ideal layer-by-layer mode at room temperature rather than at higher temperature [6, 7].

Magnetite (Fe₃O₄) is a famous half-metallic ferrimagnet, which has high Curie temperature (858 K) [8] and high spin polarization (nearly 100%) [9]. Its potential application to

serve as a ferromagnetic layer in spintronics devices, such as spin valve and magnetic tunnelling junctions (MTJs), attracts a lot of attention to the investigation of epitaxial Fe₃O₄ films [10, 11]. Epitaxial Fe₃O₄ films have been generally prepared by PLD, molecular beam epitaxy (MBE) and magnetron sputtering [12–14]. In the course of the research on Fe₃O₄ film materials, some anomalous physical properties of epitaxial Fe₃O₄ films deviating from bulk materials, for example, superparamagnetic behaviour of ultrathin films [15], unsaturated magnetization in high field [16], thickness-dependence of film resistivity [17], have drawn extra interest. In general, these properties are always attributed to a natural growth defect—antiphase domain boundaries (APBs), which are not found in the Fe₃O₄ bulk [15–17]. However, almost all of the Fe₃O₄ film samples used in the above research works were fabricated at higher substrate temperature. In this paper, we report the room-temperature layer-by-layer epitaxial growth of Fe₃O₄ thin films with a thickness ranging from 2 to 200 unit cells (u.c.) on α -Al₂O₃ substrates. The structural, electrical and magnetic properties of the Fe₃O₄ thin films were studied in detail. The experimental results show that the room-temperature epitaxial Fe₃O₄ thin films not only have similar

physical properties to those of the Fe_3O_4 films fabricated at high temperature but also have atom-level-smooth surfaces. The physical properties of the Fe_3O_4 thin films are strongly dependent on the film thickness.

2. Experimental details

A series of Fe_3O_4 thin films with various thicknesses from 2 to 200 u.c. layers were epitaxially grown on $\alpha\text{-Al}_2\text{O}_3(0001)$ substrates by laser molecular beam epitaxy (Laser-MBE) [18]. The base pressure of the epitaxy chamber was 1×10^{-5} Pa. A high-purity iron ingot (>99.99%) was used as target. The target-to-substrate distance was fixed at 70 mm. Commercial $\alpha\text{-Al}_2\text{O}_3(0001)$ substrates were annealed in air at 1200 °C for 2 h in advance to obtain the step-and-terrace surface structure. The beam of a XeCl excimer laser (308 nm, 20 ns, 2 Hz) was focused on the iron target with an energy density of about 1.5 J cm^{-2} . During the entire preparation process, the substrates were kept at room temperature ($\sim 300 \text{ K}$), and the oxygen pressure was maintained at 1×10^{-3} Pa.

The growth process of each Fe_3O_4 film was monitored by *in situ* real time reflection high-energy electron diffraction (RHEED). The RHEED monitor provides us with useful information about the thickness and the surface structure of the Fe_3O_4 films. The RHEED intensity oscillations enable us to control the film thickness exactly. The crystal structures of the films were characterized by x-ray diffraction (XRD) with $\text{Cu K}\alpha$ radiation. The Fe 2p core-level spectra were checked using x-ray photoelectron spectroscopy (XPS) with $\text{Mg K}\alpha$ radiation. Surface morphology was scanned by an atomic force microscope (AFM). The resistance measurements were carried out by the standard four-probe method using a Keithley 2400 SourceMeter. The resistivity versus temperature curve was measured by a physical property measurement system (Quantum Design, PPMS-9 T). Magnetic domains were observed with a magnetic force microscopy (MFM). Magnetic hysteresis loops were measured by vibrating sample magnetometry (VSM, PPMS-9 T).

3. Results and discussion

3.1. Structural properties

Figure 1 displays the *in situ* RHEED intensities of a specularly reflected beam as a function of growth time for the Fe_3O_4 films with thickness of 2 u.c., 5 u.c., 8 u.c., 10 u.c., 20 u.c. and 40 u.c., respectively. The clear RHEED intensity oscillations demonstrate the perfect two-dimensional (2D) layer-by-layer growth, and show the exact u.c. layer numbers of the films. We can evaluate the average growth rate is about 60 laser pulses per u.c. layer from the RHEED intensity oscillation curves. The inset of figure 1 shows a typical RHEED pattern of Fe_3O_4 films, and the RHEED pattern keeps unchanged even though the thickness reached 200 u.c. layers. The bright RHEED streaks and the uninterrupted RHEED intensity oscillation indicate that the Fe_3O_4 films can maintain a very smooth surface during the epitaxial growth. The presence of $(1/2, 1/2)$ -type rods in the RHEED pattern indicates the formation of the inverse spinel

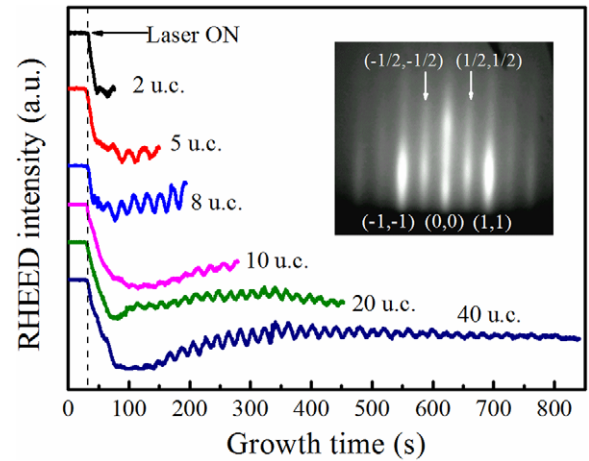


Figure 1. RHEED intensity oscillations during the room-temperature epitaxial growth of Fe_3O_4 films on $\alpha\text{-Al}_2\text{O}_3(0001)$. The inset shows a typical RHEED pattern of the Fe_3O_4 film.

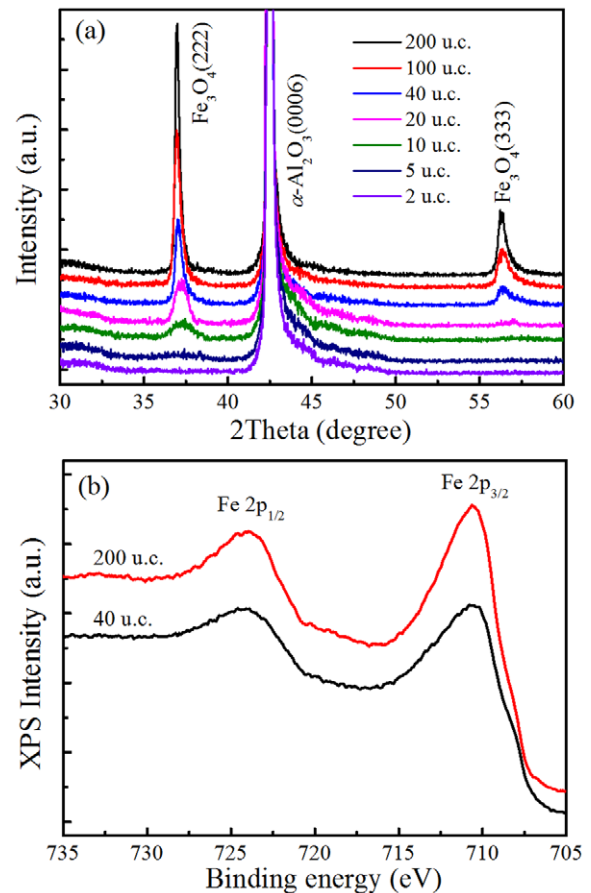


Figure 2. (a) XRD θ - 2θ profiles of Fe_3O_4 films with the thickness of 2 u.c., 5 u.c., 10 u.c., 20 u.c., 40 u.c., 100 u.c. and 200 u.c. layers, respectively. (b) Fe 2p core-level XPS spectra of 40 u.c. and 200 u.c. Fe_3O_4 films.

structure for the Fe_3O_4 film [19]. In addition, the RHEED streaky pattern reappears after rotating the substrate by 120° , implying a threefold symmetry axis of the Fe_3O_4 film, which may correspond to the $[111]$ crystal axis.

Figure 2(a) shows the XRD θ - 2θ profiles for the Fe_3O_4 films with thicknesses of 2, 5, 10, 20, 40, 100 and 200 u.c.

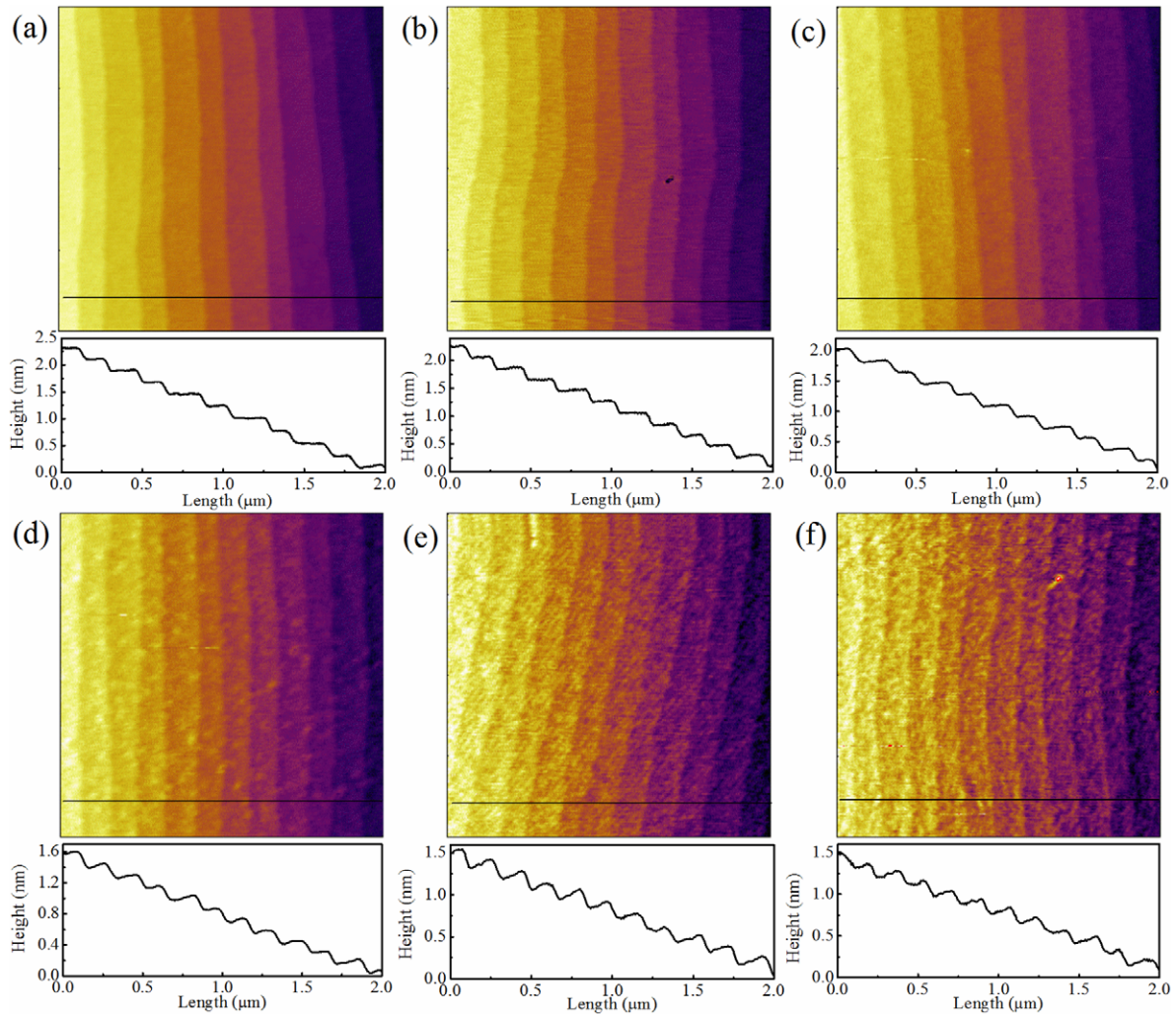


Figure 3. AFM 2D images ($2 \times 2 \mu\text{m}^2$) and the corresponding height profiles along the solid lines in the 2D images of the Al_2O_3 substrate and the Fe_3O_4 films: (a) Al_2O_3 substrate; (b)–(f) 2 u.c., 10 u.c., 40 u.c., 100 u.c. and 200 u.c. Fe_3O_4 film, respectively.

grown on $\alpha\text{-Al}_2\text{O}_3(0001)$ substrates. Only the peaks corresponding to the $\alpha\text{-Al}_2\text{O}_3(0006)$ and $\text{Fe}_3\text{O}_4(hh h)$ planes are detected, with no trace of other diffraction peaks from either secondary phase or randomly oriented grain. This means that the Fe_3O_4 thin films are single phase and high-oriented, and the epitaxial relationship is $\text{Fe}_3\text{O}_4(111) \parallel \alpha\text{-Al}_2\text{O}_3(0001)$. It should be noted that, compared with the $\alpha\text{-Al}_2\text{O}_3(0006)$ peak, the Fe_3O_4 diffraction peaks gradually shift to the high-degree direction with decreasing film thickness when the thickness is less than 100 u.c., meaning that the lattice near the interface was expanded in the (111) plane. The lattice parameter of $\alpha\text{-Al}_2\text{O}_3$ is $a = 4.76 \text{ \AA}$, whereas the surface unit cell constant is 5.92 \AA for the $\text{Fe}_3\text{O}_4(111)$ plane. Gota *et al* [19] believe the epitaxial growth of Fe_3O_4 on $\alpha\text{-Al}_2\text{O}_3$ is guided by lattice symmetry, they also observed a similar expansion of Fe_3O_4 on the $\alpha\text{-Al}_2\text{O}_3$ substrate prepared by MBE.

Figure 2(b) shows the typical Fe 2p core-level spectra of Fe_3O_4 films with 40 and 200 u.c. obtained by XPS. The binding energies of Fe $2p_{3/2}$ and Fe $2p_{1/2}$ are located at around 711 eV and 724 eV, respectively. The values are very consistent with

those of the Fe_3O_4 films fabricated at a higher temperature [20, 21]. The results point out the formation of Fe_3O_4 prepared at room temperature.

Figure 3 shows the surface morphologies of the Al_2O_3 substrate and the Fe_3O_4 films. Figure 3(a) is a two-dimensional (2D) AFM image of the as-processed $\alpha\text{-Al}_2\text{O}_3(0001)$ substrate in $2 \times 2 \mu\text{m}^2$. The step-and-terrace structure on the Al_2O_3 surface is very clear and the average step height corresponds to the spacing of $\alpha\text{-Al}_2\text{O}_3(0006)$ planes (0.216 nm). Figures 3(b)–(f) display the 2D AFM images ($2 \times 2 \mu\text{m}^2$) and height profiles for the Fe_3O_4 films with thicknesses of 2 u.c., 10 u.c., 40 u.c., 100 u.c. and 200 u.c., respectively. We can see that the surfaces of the Fe_3O_4 films maintain the original surface structures of the Al_2O_3 substrates very well. The corresponding root-mean-square (rms) surface roughness within a $2 \times 2 \mu\text{m}^2$ area is 0.088 nm, 0.083 nm, 0.095 nm, 0.116 nm, 0.109 nm and 0.129 nm for the Fe_3O_4 films with thicknesses of 2 u.c., 10 u.c., 40 u.c., 100 u.c. and 200 u.c., respectively. Just as expected, the room-temperature epitaxy of Fe_3O_4 films maintains the layer-by-layer epitaxial growth mode and the atomic scale smooth surfaces.

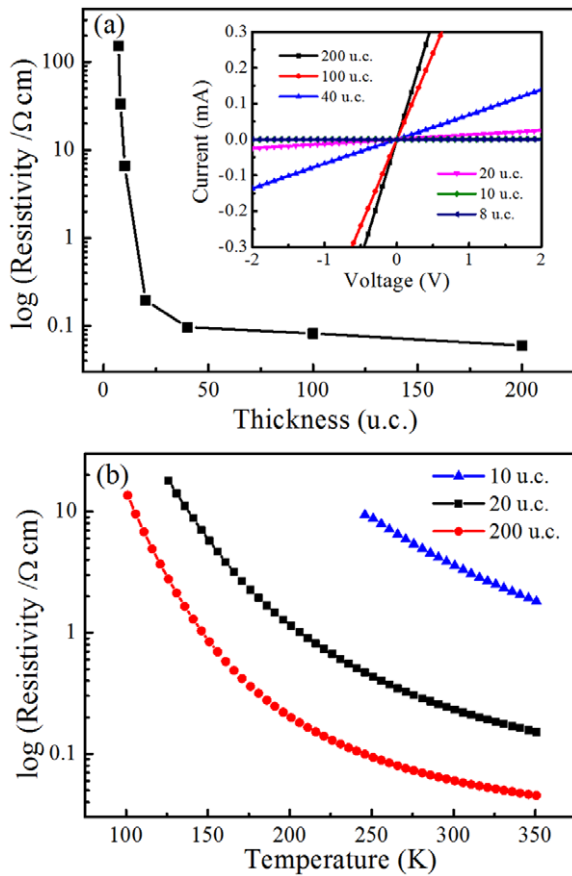


Figure 4. (a) The relation between resistivity and thickness of Fe_3O_4 films measured at room temperature. The inset presents the I - V curves of Fe_3O_4 films with thicknesses of 8 u.c., 10 u.c., 20 u.c., 40 u.c., 100 u.c. and 200 u.c. at room temperature. (b) The temperature-dependent resistivity for Fe_3O_4 films with thicknesses of 10, 20 and 250 u.c.

3.2. Electrical properties

For the measurements of electrical properties, four indium electrodes were contacted on every Fe_3O_4 film. First, we measured the contact property between Fe_3O_4 films and the indium electrodes with two electrodes at room temperature. The inset of figure 4(a) presents the current-voltage (I - V) curves of Fe_3O_4 films with thicknesses of 8, 10, 20, 40, 100 and 200 u.c. The linear I - V characteristics in figure 4(a) indicate that the contacts between Fe_3O_4 films and indium electrodes are good ohmic. Figure 4(a) shows the resistivity as a function of thickness of Fe_3O_4 films obtained at room temperature. The resistivity is too high to be measured when the thickness is less than 7 u.c. layers, and it decreases rapidly with the increase in film thickness from 7 to 12 u.c. layers. The resistivity values are 152 Ω cm, 33 Ω cm, 6.5 Ω cm, 0.19 Ω cm, 0.096 Ω cm, 0.082 Ω cm and 0.06 Ω cm for the Fe_3O_4 films with thickness of 7 u.c., 8 u.c., 10 u.c., 20 u.c., 40 u.c., 100 u.c. and 200 u.c. layers, respectively. For the thinner Fe_3O_4 films, the 7–20 u.c. layers (about 3.4–9.7 nm), the resistivity is higher than that of 0.13 Ω cm for 3 nm thick film and 0.017 Ω cm for 12 nm thick film grown at a substrate temperature of 250 $^\circ\text{C}$ reported by Eerenstein *et al* [17]. However, the resistivities of 100 and 200 u.c. (\sim 48 and 96 nm) films grown at room

temperature have the same order as Gong's reported value of \sim 0.03 Ω cm for the 150 nm thick Fe_3O_4 film deposited at a substrate temperature of 350 $^\circ\text{C}$ [22].

The resistivity of the Fe_3O_4 film decreasing with increasing thickness is a universal phenomenon that has also been observed in Fe_3O_4 (100), (111) and (110) epitaxial films grown by PLD or MBE [17, 23, 24]. It has been well accepted that APBs play a very important role in such a thickness-dependent property. At most APBs, the superexchange interactions across the boundaries are antiferromagnetic (AF) [17]. It is worth noting that Fe_3O_4 has nearly full spin polarization [25, 26]. So, these AF APBs work as barriers for the polarized conduction electrons. As a result, the presence of APBs enhances the resistivity of the film. According to the magnetic force microscope (MFM) measurements in figure 5, the density of APBs increases with reducing thickness, which means the block behaviour for conduction electrons is more serious in thinner films. As a result, the resistivity in thinner films should be higher than in thicker films. Furthermore, we consider the influence of lattice distortion at the interface cannot be ignored. Because the Fe_3O_4 crystal lattices close to the interface expand in the (1 1 1) plane, the length of the in-plane Fe–O–Fe bond is elongated. In consequence, the activation energy (the energy required for the electrons to transfer from Fe^{2+} to Fe^{3+}) is improved. As the film thickness increases, the lattice distortion relaxes gradually back to the normal state. Thus, the in-plane resistivity reduces with increasing thickness of the Fe_3O_4 film.

Figure 4(b) shows the temperature-dependent resistivity (ρ - T) for Fe_3O_4 films with the thicknesses of 10, 20 and 250 u.c. in the temperature range 100–350 K. The resistivity is low at high temperatures, and increases drastically as the temperature cools down. The evolution of the metal-insulator transition (MIT) was observed at about 130 K, 165 K and 280 K for 250 u.c., 20 u.c. and 10 u.c. films, respectively. A typical feature of Fe_3O_4 is the Verwey transition at the temperature of \sim 120 K, where an abrupt jump appears in the ρ - T curve [27]. But we do not observe the discontinuous change in the measured ρ - T curves. It seems that the Verwey transition is unlikely to be observed in ultrathin Fe_3O_4 films [17], because it is very sensitive to defects, residual strain and pressure [28, 29].

3.3. Magnetic properties

One of the typical properties of Fe_3O_4 epitaxial films is the thickness-dependent density of APBs [17, 23]. We observed the domain structures of the room-temperature epitaxial Fe_3O_4 films. Figures 5(a)–(d) present the MFM images of 200 u.c., 100 u.c., 40 u.c. and 20 u.c. films in the area of $2 \times 2 \mu\text{m}^2$, respectively. One can see that the irregular magnetic domains are very clear in the thicker films, but very obscure in the film of 20 u.c.. With regard to the thinner films, when thickness is less than 20 u.c., we cannot observe obvious domain structures. This may be due to the weak magnetism or tiny domains. In other words, the domain size decreases with decreasing film thickness.

The solid curves in figures 6(a)–(f) present the magnetic hysteresis (M - H) loops of the 200, 100, 40, 20, 10 and

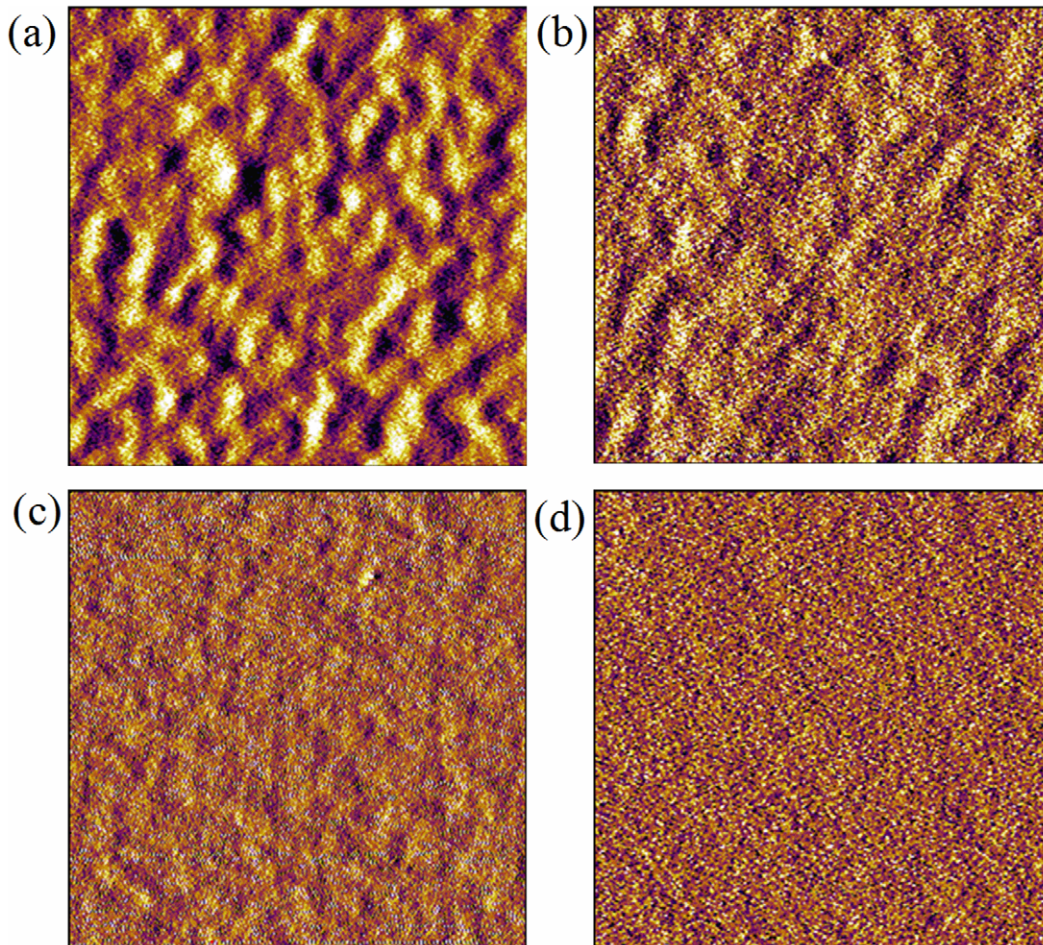


Figure 5. MFM images of Fe_3O_4 films with the thicknesses of (a) 200 u.c., (b) 100 u.c., (c) 40 u.c. and (d) 20 u.c..

5 u.c. Fe_3O_4 films measured at 10 and 300 K with the external fields parallel to the film planes. Except for the 2 u.c. Fe_3O_4 film, which shows non-magnetism, all of the other films show obvious ferromagnetism. The saturation magnetization (M_S) values are approximately 215 emu cm^{-3} , 210 emu cm^{-3} , 80 emu cm^{-3} , 50 emu cm^{-3} , 40 emu cm^{-3} and 40 emu cm^{-3} at 300 K for the films of 200 u.c., 100 u.c., 40 u.c., 20 u.c., 10 u.c. and 5 u.c., respectively. The M_S values are smaller than that of bulk Fe_3O_4 ($\sim 477 \text{ emu cm}^{-3}$). The M_S value decreases with reducing film thickness due to the increase in APBs density [17, 30].

The exchange bias (EB) effect is very likely to be observed when the system is cooled down through the Néel point of AF part with an external field if a system contains both FM and AF ingredients. In order to prove whether exchange coupling occurs in the room-temperature epitaxial Fe_3O_4 films, we measured the field-cooled (FC) $M-H$ loops at 10 K. The films were cooled from 300 to 10 K with a 5 kOe magnetic field parallel to the film plane. The short dashed curves in figure 6 also show the FC $M-H$ loops of 200, 100, 40, 20, 10 and 5 u.c. Fe_3O_4 films. It is very clear that the FC $M-H$ loops are asymmetric and shift to the negative field direction, which is a typical property of the EB effect. The EB field (H_E) reflects the shift magnitude of the $M-H$ loop, which is defined as $H_E = |H_{C-} + H_{C+}|/2$, where H_{C-} and H_{C+} are

the coercivities in the negative and positive field direction, respectively. According to the FC $M-H$ loops, H_E values are 735 Oe, 750 Oe, 969 Oe, 977 Oe and 1003 Oe for 200 u.c., 100 u.c., 40 u.c., 20 u.c. and 10 u.c. film, respectively. In comparison with the zero-field-cooled (ZFC) $M-H$ loops at 10 K in figure 6, the coercive fields of the FC $M-H$ loops are apparently enlarged. This is another property of the EB effect. The EB effect observed in the room-temperature epitaxial Fe_3O_4 films is similar to that of the Fe_3O_4 films fabricated at higher temperature [16, 31].

4. Conclusions

In summary, we have successfully grown epitaxial $\text{Fe}_3\text{O}_4(111)$ ultrathin films on $\alpha\text{-Al}_2\text{O}_3(0001)$ substrates by laser-MBE at room temperature. The room-temperature epitaxy of Fe_3O_4 films has very good repeatability. The measurements of RHEED, XRD and AFM reveal that the room-temperature epitaxial Fe_3O_4 films have high crystal quality and ultra-smooth surface. The structural, electrical and magnetic properties of the films are strongly dependent on the film thickness. The resistivity reduces with increasing film thickness. Meanwhile, saturation magnetization increases with increasing film thickness. All of the experimental results demonstrate that the

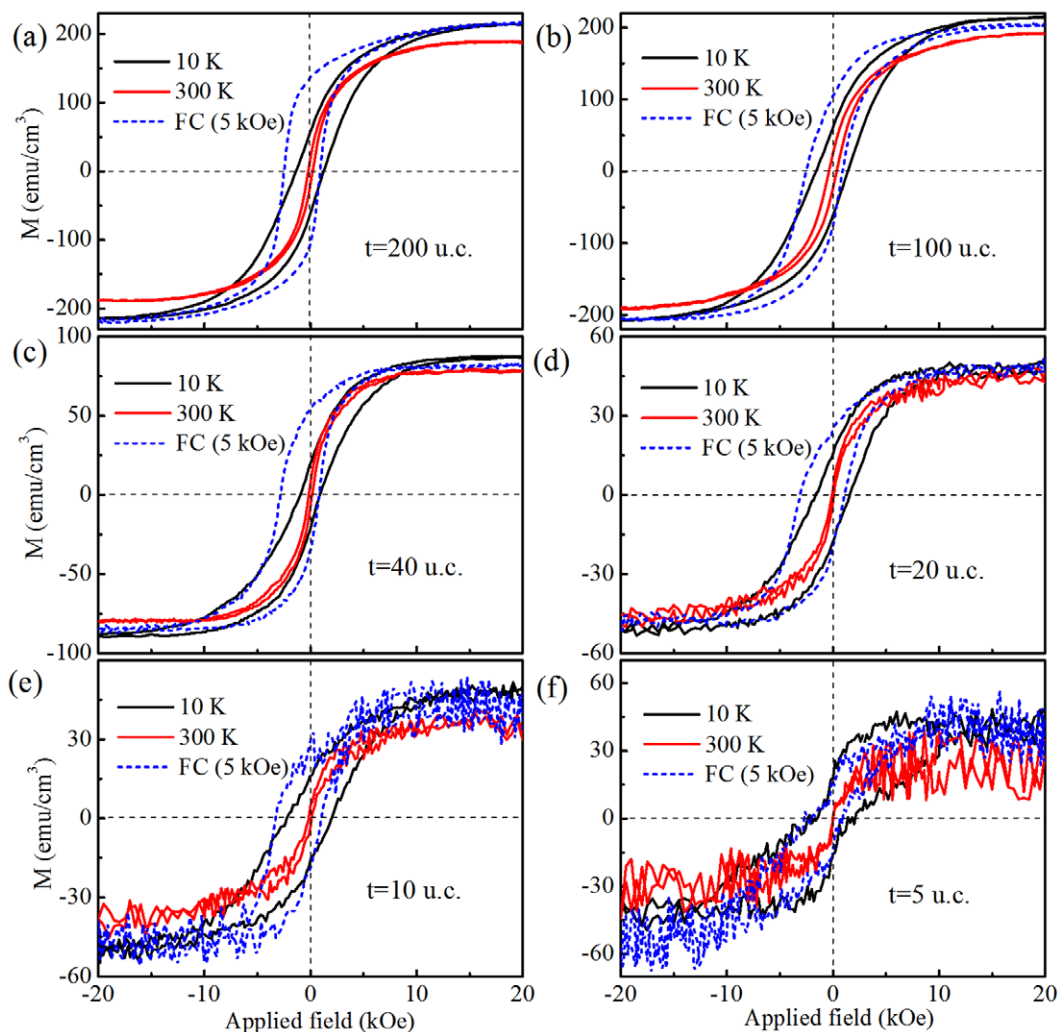


Figure 6. The magnetic hysteresis (M – H) loops of Fe_3O_4 films with the thickness of (a) 200 u.c., (b) 100 u.c., (c) 40 u.c., (d) 20 u.c., (e) 10 u.c. and (f) 5 u.c. The solid curves are M – H loops measured at 10 and 300 K, and the short dashed curves are field-cooled M – H loops measured at 10 K with a cooled field of 5 kOe.

room-temperature epitaxial Fe_3O_4 thin films have similar physical properties to the films fabricated at higher temperature [16, 17, 19–31]. In addition, the Fe_3O_4 thin films are able to tolerate strong cleaning with ultrasonics or cotton balls, implying that the Fe_3O_4 films have good binding property with the α - Al_2O_3 substrates. The results suggest that the room-temperature layer-by-layer epitaxial Fe_3O_4 films have great potential applications in functional heterostructures, magnetic electrode materials and magnetic tunnel junctions, etc.

Acknowledgment

This work was supported by the National Basic Research Program of China (Project Nos 2010CB630704 and 2012CB921403).

References

- [1] Kim M H, Oshima M, Kinoshita H, Shirakura Y, Miyamura K, Ohta J, Kobayashi A and Fujioka H 2006 *Appl. Phys. Lett.* **89** 031916
- [2] Kobayashi A, Kawano S, Kawaguchi Y, Ohta J and Fujioka H 2007 *Appl. Phys. Lett.* **90** 041908
- [3] Kajima T, Kobayashi A, Ueno K, Shimamoto K, Fujii T, Ohta J, Fujioka H and Oshima M 2010 *Japan. J. Appl. Phys.* **49** 070202
- [4] Kim M, Ohta J, Kobayashi A, Fujioka H and Oshima M 2007 *Appl. Phys. Lett.* **91** 151903
- [5] Kawaguchi Y, Ohta J, Kobayashi A and Fujioka H 2005 *Appl. Phys. Lett.* **87** 221907
- [6] Ueno K, Kobayashi A, Ohta J and Fujioka H 2007 *Appl. Phys. Lett.* **90** 141908
- [7] Shimamoto K, Kobayashi A, Mitamura K, Ueno K, Ohta J, Oshima M and Fujioka H 2010 *Japan. J. Appl. Phys.* **49** 080202
- [8] Walz F 2002 *J. Phys.: Condens. Matter* **14** 285
- [9] Zhang Z and Satpathy S 1991 *Phys. Rev. B* **44** 13319
- [10] Dijken S, Fain X, Watts S M and Coey J M D 2004 *Phys. Rev. B* **70** 052409
- [11] Hu G and Suzuki Y 2002 *Phys. Rev. Lett.* **89** 276601
- [12] Ogale S B, Ghosh K, Sharma R P, Greene R L, Ramesh R and Venkatesan T 1998 *Phys. Rev. B* **57** 7823
- [13] Anderson J F, Kuhn M, Diebold U, Shaw K, Stoyanov P and Lind D 1997 *Phys. Rev. B* **56** 9902
- [14] Balakrishnan K, Arora S K and Shvets I V 2004 *J. Phys.: Condens. Matter* **16** 5387

- [15] Vooge F C, Palstra T T M, Niesen L, Rogojanu O C, James M and Hibma T 1998 *Phys. Rev. B* **57** R8107
- [16] Margulies D T, Parker F T, Spada F E, Goldman R S, Li J, Sinclair R and Berkowitz A E 1996 *Phys. Rev. B* **53** 9175
- [17] Eerenstein W, Palstra T T M, Hibma T and Celotto S 2002 *Phys. Rev. B* **66** 201101(R)
- [18] Yang G Z, Lu H B, Chen F, Zhao T and Chen Z H 2001 *J. Cryst. Growth* **227–228** 929
- [19] Gota S, Moussy J-B, Henriot M, Guittet M-J and Gautier-Soyer M 2001 *Surf. Sci.* **482–485** 809
- [20] Wong P K J, Zhang W, Cui X G, Xu Y B, Wu J, Tao Z K, Li X, Xie Z L, Zhang R, van der Laan G 2010 *Phys. Rev. B* **81** 035419
- [21] Fujii T, de Groot F M F, Sawatzky G A, Vooge F C, Hibma T and Okada K 1999 *Phys. Rev. B* **59** 3195
- [22] Gong G Q, Gupta A, Xiao G, Qian W and Dravid V 1997 *Phys. Rev. B* **56** 5096
- [23] Moussy J-B *et al* 2004 *Phys. Rev. B* **70** 174448
- [24] Sofin R G S, Arora S K and Shvets I V 2011 *Phys. Rev. B* **83** 134436
- [25] Alvarado S F, Eib W, Meier F, Pierce D T, Sattler K, Siegmann H C and Remeika J P 1975 *Phys. Rev. Lett.* **34** 319
- [26] Dedkov Yu S, Rudiger U and Guntherodt G 2002 *Phys. Rev. B* **65** 064417
- [27] Verwey E J W 1939 *Nature* **144** 327
- [28] Jain S, Adeyeye A O and Boothroyd C B 2005 *J. Appl. Phys.* **97** 093713
- [29] Lai C, Hung P, Wang Y and Huang R T 2004 *J. Appl. Phys.* **95** 7222
- [30] Bobo J F *et al* 2001 *Eur. Phys. J. B* **24** 43
- [31] Arora S K, Sofin R G S, Nolan A and Shvets I V 2005 *J. Magn. Magn. Mater.* **286** 463